The Canadian Journal of Mineralogy and Petrology
ISSN 2817-1713
Vol. 61, pp. 987-998 (2023)
DOI: 10.3749/2300004

PETERMEGAWITE, $Al_6(Se^{4+}O_3)_3[SiO_3(OH)](OH)_9 \cdot 10H_2O$, A NEW Al-BEARING SELENITE MINERAL, FROM THE EL DRAGÓN MINE, POTOSÍ, BOLIVIA

HEXIONG YANG[§]

Department of Geosciences, University of Arizona, 1040 E. 4th Street, Tucson, Arizona 85721-0077, USA

XIANGPING GU

School of Geosciences and Info-Physics, Central South University, #932, South Lushan Road, Changsha, Hunan 410083, China

MICHAEL M. SCOTT, ROBERT A. JENKINS, RONALD B. GIBBS, JAMES A. MCGLASSON, AND ROBERT T. DOWNS

Department of Geosciences, University of Arizona, 1040 E. 4th Street, Tucson, Arizona 85721-0077, USA

ABSTRACT

A new mineral species, petermegawite, ideally $Al_6(Se^{4+}O_3)_3[SiO_3(OH)](OH)_9 \cdot 10H_2O$, was discovered at the El Dragón mine, Potosí Department, Bolivia. It occurs as aggregates of bladed or tabular crystals. Associated minerals are Co-bearing krut′aite–penroseite (matrix), chalcomenite, 'clinochalcomenite' (not IMA approved), molybdomenite, lepidocrocite, goethite, ahlfeldite, and calcite. Petermegawite is colorless in transmitted light and transparent with a white streak and vitreous luster. It is brittle and has a Mohs hardness of 2–2½. Cleavage is perfect on {001}. The measured and calculated densities are 2.27(5) and 2.32 g/cm^3, respectively. Optically, petermegawite is biaxial (+), with $\alpha = 1.545(5)$, $\beta = 1.554(5)$, $\gamma = 1.567(5)$ (white light). An electron microprobe analysis yielded an empirical formula (based on 10 non-H cations *pfu*) of $Al_{6.00}[(Se_{0.89}S_{0.11})_{\Sigma 1.00}O_3]_3[(Si_{0.90}Al_{0.07})_{\Sigma 0.97}O_{2.81}(OH)_{1.19}](OH)_9 \cdot 10H_2O$, which can be simplified to $Al_6[(Se,S)O_3]_3[(Si,Al)O_3(OH)](OH)_9 \cdot 10H_2O$.

Petermegawite is orthorhombic, space group $Cmc2_1$ with unit-cell parameters $a = 16.2392(2)$, $b = 10.96370(10)$, $c = 15.3367(2)$ Å, $V = 2730.57(5)$ Å^3, and $Z = 4$. Its crystal structure is characterized by clusters of six-membered rings of edge-sharing AlO_6 octahedra with an $SiO_3(OH)$ tetrahedron situated at the center of each ring and three $Se^{4+}O_3$ triangular pyramids appended outside the ring. These clusters are joined together by hydrogen bonds to form heteropolyhedral layers parallel to (001). The H_2O molecules that are not bonded to any non-H cations are sandwiched between the layers. The cluster formed by a six-membered AlO_6 octahedral ring with an SiO_3OH tetrahedron at the center of the ring in petermegawite has the composition $[Al_6(SiO_3OH)O_6(OH)_9(H_2O)_6]^{6-}$. It is topologically identical to the clusters of composition $[Al_6(AsO_4)O_7(OH)_9(H_2O)_5]^{8-}$ that are found in bettertonite and penberthycroftite. As a new polyoxometalate building block, this type of cluster may be expressed with a general chemical formula $[TM_6X_{25}]$, where T = tetrahedrally coordinated cation, M = octahedrally coordinated cation, and X = O, OH, H_2O.

Keywords: petermegawite, aluminum selenite, new mineral, crystal structure, Raman, El Dragón mine.

INTRODUCTION

In recent years, there has been a growing interest in selenites as a class of compounds having novel technological applications. This is due to the fact that when heated under reducing conditions, the selenides that form possess several interesting optical, magnetic, and photoelectric or semi-conductor properties (Yankova *et al.* 2021 and references therein). Environmentally, both selenite $(Se^{4+}O_3)^{2-}$ and selenate $(Se^{6+}O_4)^{2-}$ species are considered to be the dominant forms of selenium present in aqueous systems (Girling 1984). Selenium can be either essential or toxic to humans, animals, and certain plants, based on its concentration

[§] *Corresponding author e-mail address*: hyang@arizona.edu

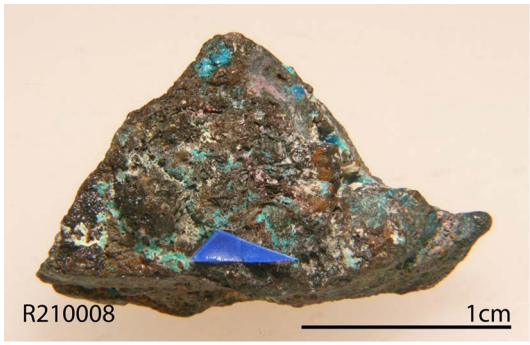

FIG. 1. The specimen on which the new mineral petermegawite (at the blue arrow) was found.

(Girling 1984, Kaur *et al.* 2014). As water-quality standards become stricter, conventional drinking-water treatments, such as coagulation, sedimentation, and filtration, are constrained in removing trace amounts of Se^{4+} and Se^{6+}. Typically, Al- and Fe^{3+}-selenite compounds serve extensively as coagulants in conventional treatment processes, given their abundance in natural environments. Therefore, considerable effort has been devoted to understanding crystal structures of different Al- and Fe^{3+}-selenites and the conditions under which they develop. While more than 10 different synthetic Fe^{3+}-selenites [*e.g.*, $FeH(SeO_3)_2$, $Fe(HSeO_3)_3$, $Fe_2(SeO_3)_3 \cdot 6H_2O$, $Fe(HSeO_3)(Se_2O_5)$, $Fe(SeO_2OH)(SeO_4) \cdot H_2O$, $Fe_2(SeO_3)_3 \cdot H_2O$, $KFe(SeO_3)_2$, $LiFe(Se_2O_5)_2$, $LiFe(SeO_3)_2$, $Fe_2(SeO_3) \cdot 3H_2O$] are known (Giester & Pertlik 1994 and references therein), only three Al-selenites, $Al_2(SeO_3)_3 \cdot 3H_2O$, $Al_2(SeO_3)_3 \cdot 6H_2O$, and $AlH(SeO_3)_2 \cdot 2H_2O$, have been synthesized and characterized (Morris *et al.* 1991, 1992, Harrison *et al.* 1992, Ratheesh *et al.* 1997). Among them, dimorphs of $Al_2(SeO_3)_3 \cdot 6H_2O$ has been found in nature: alfredopetrovite, which is hexagonal ("$P\bar{6}2c$"; Kampf *et al.* 2016a), and bernardevansite, which is monoclinic ($P2_1/c$; Yang *et al.* 2022a). In this study, we report on a third Al-selenite mineral, petermegawite, ideally $Al_6(SeO_3)_3[SiO_3(OH)](OH)_9 \cdot 10H_2O$, which was discovered at the El Dragón mine, Bolivia.

The new mineral, petermegawite, is named in honor of Dr. Peter K.M. Megaw, who earned his Ph.D. in geology from the University of Arizona in 1990 and is a consulting geologist, President of IMDEX/Cascabel, and co-founder of MAG Silver and Minaurum Gold. Dr. Megaw has been a dedicated mineral collector since 1977. After moving to Tucson in 1979, he took on the job of the Exhibits Chair for the Tucson Gem and Mineral Show in 1984. His mineral collecting has come to focus almost exclusively on minerals of Mexico, and he has spoken and written extensively on specimen localities there. Dr. Megaw is also a contributing editor for journals including *Rocks and Minerals* and occasionally writes for *Mineralogical Monographs, Mineral News, Mineralien Welt, Extra Lapis*, and *Mineral Observer*. In his spare time, he collaborates on studies of silver isotopes in silver minerals. He is Mindat's (https://www.mindat.org/) moderator for submissions on Mexico and co-moderator of the FMF Mineral Forum. A combination of the above led him to be awarded the Carnegie Mineralogical Award for 2009. In 2010, Dr. Megaw and his family, together with the Philadelphia Academy of Sciences, rescued the collection of the American Philosophical Society, the oldest coherent mineral collection in the U.S., from commercial dispersal following its sale and donated it to the Smithsonian Institution. Dr. Megaw has also made numerous donations to mineral museums around the world, including Harvard, New Mexico Tech, Natural History Museum London, and the University of Arizona. The new mineral and its name have been approved by the Commission on New Minerals, Nomenclature and Classification (CNMNC) of the International Mineralogical Association (IMA 2021-079). The co-type samples have been deposited at the University of Arizona Alfie Norville Gem and Mineral Museum (Catalogue # 22711) and the RRUFF Project (deposition # R210008) (http://rruff.info).

Sample Description and Experimental Methods

Occurrence

Petermegawite was found on a specimen (Fig. 1) collected from the El Dragón mine (19°49′15″S, 65°55′0″W), Antonio Quijarro Province, Potosí Department, Bolivia. Associated minerals include Co-bearing krut′aite–penroseite (matrix), chalcomenite, 'clinochalcomenite' (not IMA

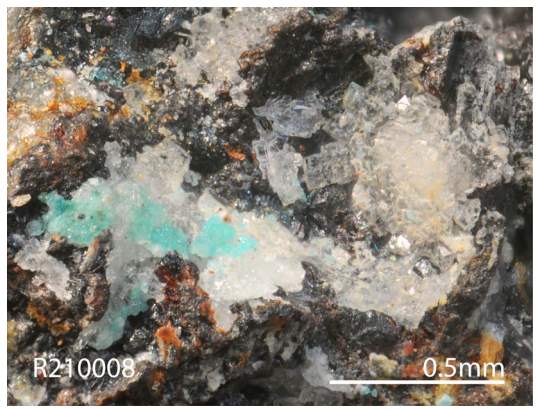

FIG. 2. A microscopic view of aggregates of colorless tabular or short bladed crystals of petermegawite. The pale green-blue mineral is 'clinochalcomenite' (not in the list of IMA approved minerals).

TABLE 1. ANALYTICAL DATA (in wt.%) FOR PETERMEGAWITE

Constituent	Mean	Range	Stand. Dev.	Probe Standard
SiO_2	5.83	5.62–6.10	0.16	SiO_2
Al_2O_3	33.21	32.29–34.31	0.68	Al_2O_3
SeO_2	31.90	31.31–33.02	0.58	CdSe
SO_2	2.35	1.95–2.61	0.21	FeS_2
H_2O	29.17			Calculated**
Total*	102.46	99.71–102.55	1.10	

* Petermegawite is prone to electron beam damage, but it did not seem to affect the relative proportions of cations. In addition, as is typical of highly hydrated phases with weakly held H_2O, petermegawite partially dehydrates under vacuum either during carbon coating or in the microprobe chamber. The combination of the above two factors results in the relatively large variation and the slightly higher total than expected for the fully hydrated phase.

** The concentration of H_2O was estimated by the stoichiometry with $(OH)^-$ anion in the anhydrous part and 10 H_2O molecules *pfu*.

approved), molybdomenite, lepidocrocite, goethite, ahlfeldite, and calcite. It is worth noting that a description of 'clinochalcomenite' was published in 1980 without the approval of the IMA-CNMNC (Lo *et al.* 1980) and the crystal-structure determination of this species was subsequently reported (Lo *et al.* 1984). Detailed descriptions of the geology and mineralogy of the El Dragón mine have been given by Grundmann *et al.* (1990, 2007) and Grundmann & Förster (2017). This mine exploited a telethermal deposit consisting of a single selenide vein hosted in sandstones and shales. The major ore mineral is krut′aite, $CuSe_2$, which ranges in composition to penroseite, $NiSe_2$. Late-stage fluid, rich in Bi, Pb, and Hg, resulted in the crystallization of minerals such as clausthalite, petrovicite, watkinsonite, and the recently described minerals eldragónite, $Cu_6BiSe_4(Se_2)$ (Paar *et al.* 2012); grundmannite, $CuBiSe_2$ (Förster *et al.* 2016); hansblockite, $(Cu,Hg)(Bi,Pb)Se_2$ (Förster *et al.* 2017); cerromojonite, $CuPbBiSe_3$ (Förster *et al.* 2018); and nickeltyrrellite, $CuNi_2Se_4$ (Förster *et al.* 2019). Oxidation produced a wide range of secondary Se-bearing minerals, such as favreauite, $PbBiCu_6O_4(SeO_3)_4(OH)\cdot H_2O$ (Mills *et al.* 2014); alfredopetrovite, $Al_2(Se^{4+}O_3)_3\cdot 6H_2O$ (Kampf *et al.* 2016a); bernardevansite, $Al_2(Se^{4+}O_3)_3\cdot 6H_2O$, dimorphous with alfredopetrovite (Yang *et al.* 2022a); franksousaite, $PbCu(Se^{6+}O_4)(OH)_2$ (Yang *et al.* 2022b); and the new mineral petermegawite, described herein.

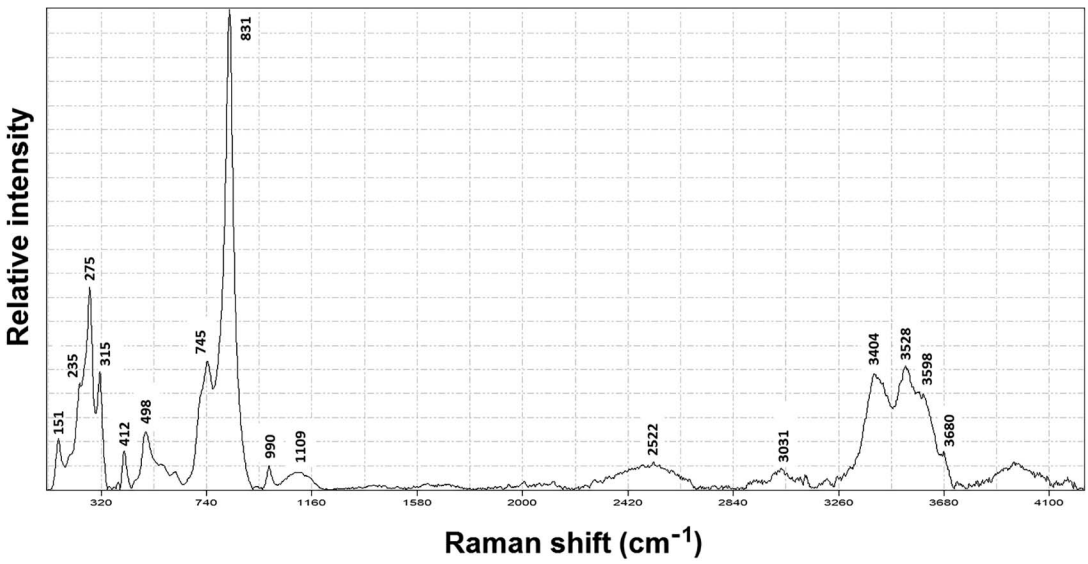

FIG. 3. The Raman spectrum of petermegawite.

TABLE 2. X-RAY POWDER DIFFRACTION data (d in Å, I in %) FOR PETERMEGAWITE

I_{calc}	I_{meas}	d_{meas}	d_{calc}	hkl	I_{calc}	I_{meas}	d_{meas}	d_{calc}	hkl
40.2	31.0	9.120	9.089	1 1 0	5.7	8.4	2.264	2.264	3 1 6
100.0	100.0	7.824	7.821	1 1 1	11.4	12.4	2.218	2.213	6 0 4
77.2	88.5	7.642	7.676	0 0 2	4.5	5.5	2.180	2.178	7 1 2
67.0	53.3	5.839	5.864	1 1 2	8.8	8.6	2.146	2.152	1 5 1
73.4	82.7	5.580	5.580	2 0 2	2.1	2.7	2.081	2.079	1 3 6
57.9	88.1	5.514	5.483	0 2 0	6.6	4.9	2.052	2.052	6 2 4
79.1	67.0	4.860	4.856	3 1 0	6.3	7.1	2.020	2.015	3 5 1
30.7	29.7	4.572	4.545	2 2 0	2.2	7.7	2.009	1.983	2 4 5
28.2	48.7	4.496	4.459	1 1 3	22.0	22.8	1.976	1.977	5 1 6
5.0	0.9	4.325	4.358	2 2 1	3.6	10.0	1.954	1.955	4 4 4
3.9	7.1	4.077	4.063	4 0 0	2.9	2.7	1.917	1.919	0 0 8
46.1	35.6	3.880	3.911	2 2 2	13.7	14.2	1.863	1.860	6 0 6
15.4	12.8	3.821	3.838	0 0 4	6.4	15.0	1.854	1.849	8 2 2
12.5	19.7	3.539	3.566	1 3 0	10.6	13.1	1.813	1.815	0 6 1
10.3	17.0	3.498	3.536	1 1 4	2.9	2.0	1.791	1.795	8 0 4
15.0	16.6	3.463	3.470	2 0 4	4.2	3.8	1.775	1.778	0 6 2
26.6	30.3	3.270	3.264	4 2 0	6.1	5.1	1.763	1.762	5 3 6
14.4	34.1	3.236	3.234	1 3 2	3.9	6.6	1.738	1.737	2 6 2
14.4	27.7	3.164	3.193	4 2 1	2.8	2.2	1.696	1.695	3 5 5
26.8	28.8	3.131	3.144	0 2 4	3.4	6.0	1.653	1.652	7 3 5
34.3	49.1	3.040	3.030	3 3 0	5.7	13.7	1.627	1.625	10 0 0
55.0	81.2	3.017	3.011	3 1 4	3.4	13.5	1.621	1.621	3 3 8
9.2	8.4	2.936	2.932	2 2 4	2.8	5.1	1.595	1.596	8 4 2
32.2	30.5	2.891	2.887	5 1 2	2.0	5.5	1.588	1.584	9 3 2
6.2	6.9	2.799	2.790	4 0 4	10.7	7.5	1.561	1.564	5 5 5
8.4	6.2	2.739	2.741	0 4 0	1.6	2.0	1.537	1.535	0 0 10
6.3	4.7	2.716	2.708	6 0 0	4.7	6.4	1.528	1.529	4 6 4
12.7	9.7	2.664	2.661	5 1 3	4.3	4.7	1.511	1.514	1 1 10
3.3	8.2	2.606	2.607	3 3 3	2.4	2.0	1.497	1.498	3 7 1
4.5	8.4	2.580	2.582	0 4 2	4.0	1.3	1.484	1.482	5 5 6
3.6	3.3	2.557	2.561	2 4 1	3.8	6.2	1.465	1.466	7 1 8
16.9	31.4	2.460	2.463	1 1 6	4.2	4.2	1.455	1.454	2 2 10
8.2	11.7	2.422	2.419	5 1 4	3.2	3.3	1.442	1.444	10 2 4
6.7	9.1	2.384	2.378	3 3 4	4.0	3.8	1.408	1.409	6 6 4
11.8	19.5	2.316	2.316	5 3 2					

Physical and chemical properties and Raman spectrum

Petermegawite occurs as aggregates of bladed or tabular crystals (Fig. 2). Individual crystals of petermegawite are up to 0.15 × 0.08 × 0.03 mm, with the common crystal forms {001}, {100}, {010}. Petermegawite is colorless in transmitted light, transparent with a white streak and vitreous luster. It is brittle and has a Mohs hardness of 2–2½. Cleavage is perfect on {001}. The density measured by flotation in heavy liquids is 2.27(5) g/cm^3, and the calculated density is 2.32 g/cm^3 on the basis of the empirical chemical formula and unit-cell volume from single-crystal X-ray diffraction data. Optically, petermegawite is biaxial (+), with $\alpha = 1.545(5)$, $\beta = 1.554(5)$, $\gamma = 1.567(5)$ (white light), $2V$ (meas.) = 77(2)°, $2V$ (calc.) = 80°. The pleochroism is very weak, from pale gray to gray, and dispersion is weak with $r > v$. The calculated compatibility index based on the empirical formula is 0.013 (superior) (Mandarino 1981). Petermegawite is insoluble in water or hydrochloric acid.

The chemical composition of petermegawite was determined using a Shimadzu-1720 electron microprobe (WDS mode, 15 kV, 10 nA, and a beam diameter of 2 μm). The standards used for the probe analysis are given in Table 1, along with the measured compositions (8 analysis points). The resultant chemical formula, calculated on the basis of 10 non-H cations *pfu* (from the structure determination), is $Al_{6.00}[(Se_{0.89}S_{0.11})_{\Sigma 1.00}O_3]_3[(Si_{0.90}Al_{0.07})_{\Sigma 0.97}O_{2.81}(OH)_{1.19}](OH)_9 \cdot 10H_2O$, which can be simplified to $Al_6[(Se,S)O_3]_3[(Si,Al)O_3(OH)](OH)_9 \cdot 10H_2O$.

TABLE 3. MINERALOGICAL AND STRUCTURE REFINEMENT STATISTICS DATA FOR PETERMEGAWITE

Ideal chemical formula	$Al_6(SeO_3)_3[SiO_3(OH)](OH)_9 \cdot 10H_2O$
Crystal symmetry	orthorhombic
Space group	$Cmc2_1$ (#36)
a (Å)	16.2392(2)
b (Å)	10.96370(10)
c (Å)	15.3367(2)
V (Å^3)	2730.57(5)
ρ_{obs}, ρ_{cal} (g/cm^3)	2.27(5), 2.32
Z	4
2θ range for data collection (Cu$K\alpha$)	≤153.80
No. of reflections collected	7918
No. of independent reflections	208
No. of reflections with $I > 2\sigma(I)$	2049
No. of parameters refined	208
R(int)	0.036
Final R_1, wR_2 factors [$I > 2\sigma(I)$]	0.041, 0.114
Goodness-of-fit	1.054

TABLE 4. FRACTIONAL ATOMIC COORDINATES AND EQUIVALENT ISOTROPIC DISPLACEMENT PARAMETERS (Å^2) FOR PETERMEGAWITE

Atom	x	y	z	U_{eq}	Occ. (<1)
Al1	0.08996 (12)	0.23870 (19)	0.16250 (15)	0.0189 (5)	
Al2	0.17931 (12)	0.0470 (2)	0.07542 (15)	0.0184 (5)	
Al3	0.08997 (12)	0.14878 (18)	0.48537 (16)	0.0188 (5)	
Se1	0.29942 (4)	0.47759 (7)	0.37382 (5)	0.0204 (3)	0.881 (11)
S1	0.29942 (4)	0.47759 (7)	0.37382 (5)	0.0204 (3)	0.119 (11)
Se2	0	0.50079 (14)	0.12422 (12)	0.0231 (4)	0.861 (14)
S2	0	0.50079 (14)	0.12422 (12)	0.0231 (4)	0.139 (14)
Si	0	0.1103 (3)	0.0013 (2)	0.0178 (6)	
O1	0.2156 (4)	0.5011 (6)	0.3139 (4)	0.0310 (14)	
O2	0.1671 (3)	0.1217 (5)	0.3928 (4)	0.0231 (12)	
O3	0.2551 (3)	0.4454 (5)	0.4731 (4)	0.0252 (11)	
O4	1/2	0.0199 (8)	0.0167 (7)	0.036 (2)	
O5	0.0827 (3)	0.4079 (5)	0.1375 (4)	0.0257 (12)	
O6	0.0826 (3)	0.0259 (4)	0.0044 (4)	0.0195 (11)	
O7	0	0.2022 (6)	0.0835 (5)	0.0195 (14)	
O8H	1/5	0.3154 (8)	0.4104 (6)	0.0285 (17)	
O9H	0	0.2433 (7)	0.2407 (5)	0.0231 (16)	
O10H	0.1726 (3)	0.2202 (5)	0.0780 (4)	0.0213 (11)	
O11H	0.1185 (3)	0.0734 (5)	0.1784 (4)	0.0229 (11)	
O12W	0.1659 (3)	0.2774 (5)	0.2556 (4)	0.0256 (11)	
O13W	0.2780 (3)	0.0433 (5)	0.1418 (4)	0.0266 (12)	
O14H	0.3311 (3)	0.3760 (5)	0.0731 (4)	0.0229 (11)	
O15H	0	0.1844 (7)	0.5596 (5)	0.0207 (15)	
O16H	0	0.1491 (7)	0.4104 (5)	0.0222 (16)	
O17W	0.1147 (3)	0.3182 (5)	0.4715 (4)	0.0275 (12)	
O18W	1/2	0.4043 (14)	0.2434 (9)	0.070 (4)	
O19W	0	0.4749 (14)	0.3198 (12)	0.132 (10)	
O20W	0.3767 (8)	0.1524 (12)	0.4266 (8)	0.103 (5)	

TABLE 5. ATOMIC DISPLACEMENT PARAMETERS (Å^2)

	U^{11}	U^{22}	U^{33}	U^{12}	U^{13}	U^{23}
Al1	0.0160 (9)	0.0215 (10)	0.0191 (11)	0.0000 (7)	−0.0002 (8)	−0.0012 (9)
Al2	0.0158 (8)	0.0223 (9)	0.0172 (11)	0.0005 (8)	0.0003 (8)	−0.0009 (9)
Al3	0.0142 (8)	0.0207 (10)	0.0214 (11)	−0.0006 (7)	0.0012 (8)	0.0005 (9)
Se1	0.0191 (4)	0.0241 (4)	0.0179 (5)	−0.0024 (2)	−0.0007 (4)	−0.0003 (4)
S1	0.0191 (4)	0.0241 (4)	0.0179 (5)	−0.0024 (2)	−0.0007 (4)	−0.0003 (4)
Se2	0.0172 (6)	0.0187 (6)	0.0335 (8)	0	0	0.0023 (4)
S2	0.0172 (6)	0.0187 (6)	0.0335 (8)	0	0	0.0023 (4)
Si	0.0115 (10)	0.0212 (13)	0.0208 (14)	0	0	−0.0051 (11)
O1	0.030 (3)	0.037 (3)	0.026 (3)	−0.006 (2)	−0.007 (3)	0.001 (3)
O2	0.018 (2)	0.025 (2)	0.026 (3)	0.0026 (18)	0.006 (2)	0.003 (2)
O3	0.021 (2)	0.030 (3)	0.025 (3)	−0.004 (2)	−0.002 (2)	0.003 (2)
O4	0.034 (4)	0.035 (4)	0.038 (6)	0	0	0.009 (4)
O5	0.021 (2)	0.023 (3)	0.033 (3)	−0.0016 (19)	0.001 (2)	0.004 (2)
O6	0.015 (2)	0.021 (2)	0.022 (3)	−0.0001 (16)	0.003 (2)	−0.002 (2)
O7	0.012 (3)	0.025 (3)	0.022 (4)	0	0	−0.002 (3)
O8H	0.026 (3)	0.035 (4)	0.025 (4)	0	0	−0.002 (3)
O9H	0.019 (3)	0.028 (4)	0.022 (4)	0	0	0.000 (3)
O10H	0.017 (2)	0.025 (2)	0.022 (3)	−0.0036 (18)	0.000 (2)	0.000 (2)
O11H	0.019 (2)	0.023 (2)	0.026 (3)	0.004 (2)	−0.001 (2)	0.002 (2)
O12W	0.026 (2)	0.028 (2)	0.023 (3)	−0.004 (2)	−0.003 (2)	0.000 (2)
O13W	0.018 (2)	0.037 (3)	0.025 (3)	0.002 (2)	0.000 (2)	0.001 (2)
O14H	0.018 (2)	0.026 (2)	0.025 (3)	−0.001 (2)	0.002 (2)	0.001 (2)
O15H	0.015 (3)	0.027 (3)	0.020 (4)	0	0	0.000 (3)
O16H	0.017 (3)	0.027 (4)	0.022 (4)	0	0	0.002 (3)
O17W	0.022 (2)	0.026 (2)	0.035 (3)	−0.003 (2)	−0.001 (2)	0.001 (2)
O18W	0.087 (9)	0.082 (9)	0.041 (7)	0	0	0.021 (7)
O19W	0.29 (3)	0.053 (9)	0.056 (10)	0	0	−0.022 (8)
O20W	0.116 (9)	0.125 (10)	0.068 (7)	−0.068 (8)	0.019 (7)	−0.033 (7)

TABLE 6. SELECTED BOND DISTANCES IN PETERMEGAWITE

	Distance (Å)		Distance (Å)
Al1–O10H	1.876(5)	Al2–O14H	1.882(5)
Al1–O11H	1.887(5)	Al2–O11H	1.885(6)
Al1–O9H	1.891(6)	Al2–O3	1.898(6)
Al1–O5	1.898(6)	Al2–O13W	1.900(6)
Al1–O12W	1.934(6)	Al2–O10H	1.903(5)
Al1–O7	1.940(5)	Al2–O6	1.925(5)
<Al1–O>	1.904	<Al2–O>	1.899
Al3–O16H	1.860(5)	Si–O7	1.614(8)
Al3–O14H	1.879(6)	Si–O8H	1.614(9)
Al3–O15H	1.893(5)	Si–O6 × 2	1.630(5)
Al3–O17W	1.913(6)	<Si–O>	1.622
Al3–O2	1.916(5)		
Al3–O6	1.941(5)		
<Al3–O>	1.900		
Se1–O1	1.662(6)	Se2–O4	1.662(11)
Se1–O2	1.696(5)	Se2–O5 × 2	1.698(5)
Se1–O3	1.720(6)		
<Se1–O>	1.693	<Se2–O>	1.686

TABLE 7. BOND-VALENCE SUMS FOR PETERMEGAWITE

	Al1	Al2	Al3	Se1	Se2	Si	SUM
O1				1.430			1.430
O2			0.449	1.303			1.752
O3		0.471		1.223			1.649
O4					1.418		1.418
O5	0.472				1.287 × 2↓		1.759
O6		0.439	0.420			0.984 × 2↓	1.843
O7	0.421 × 2 →					1.028	1.871
O8H						1.027	1.027
O9H	0.481 × 2→						0.962
O10H	0.501	0.465					0.966
O11H	0.486	0.488					0.975
O12W	0.428						0.428
O13W		0.470					0.470
O14H		0.493	0.497				0.990
O15H			0.478 × 2→				0.956
O16H			0.523 × 2→				1.047
O17W			0.453				0.453
O18W							
O19W							
O20W							
SUM	2.790	2.826	2.821	3.956	3.992	4.023	

Note: The bond-valence sums for Se1 and Se2 were calculated based on (0.88 Se^{4+} + 0.12 S^{4+}) and (0.86 Se^{4+} + 0.14 S^{4+}), respectively.

The Raman spectrum of petermegawite (Fig. 3) was collected on a randomly oriented crystal with a Thermo Almega microRaman system using a solid-state laser with a wavelength of 532 nm at 50% of 150 mW power (because the sample was burned by the laser at the full power) and a thermoelectric cooled CCD detector. The laser is partially polarized with 4 cm^{-1} resolution and a spot size of 1 μm. Details of the spectrum are discussed below.

X-ray crystallography

Both the powder and single-crystal X-ray diffraction data for petermegawite were collected on a Rigaku Xtalab Synerg D/S 4-circle diffractometer equipped with Cu$K\alpha$ radiation. Powder X-ray diffraction data were collected in the Gandolfi powder mode at 50 kV and 1 mA (Table 2) and the unit-cell parameters were refined using the program by Holland & Redfern (1997): a = 16.2501(4), b = 10.9652(3), c = 15.3516(4) Å, and V = 2735.47(9) $Å^3$.

Single-crystal X-ray diffraction data of petermegawite were collected from a 0.03 × 0.02 × 0.02 mm fragment. The systematic absences of reflections suggest possible space groups $Cmc2_1$, $C2cm$, or $Cmcm$. The structure was solved and refined using SHELX2018 (Sheldrick 2015a, b) based on space group $Cmc2_1$ because it produced better refinement statistics in terms of bond lengths and angles, atomic displacement parameters, and R factors. A preliminary refinement on the ratios of Se *versus* S at the *Se*1 and *Se*2 sites shows a similar preference of S for the two sites: 0.119(10) S at the *Se*1 site and

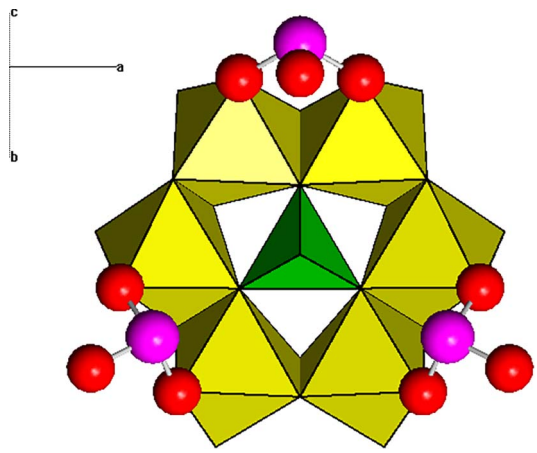

FIG. 4. The crystal structure of petermegawite showing a cluster of a six-membered ring of edge-shared AlO_6 octahedra, with an $SiO_3(OH)$ tetrahedron at the center of the ring and three $Se^{4+}O_3$ triangular pyramids appended outside. The yellow octahedra, green tetrahedron, purple spheres, and red spheres represent AlO_6, $SiO_3(OH)$, Se, and O atoms, respectively.

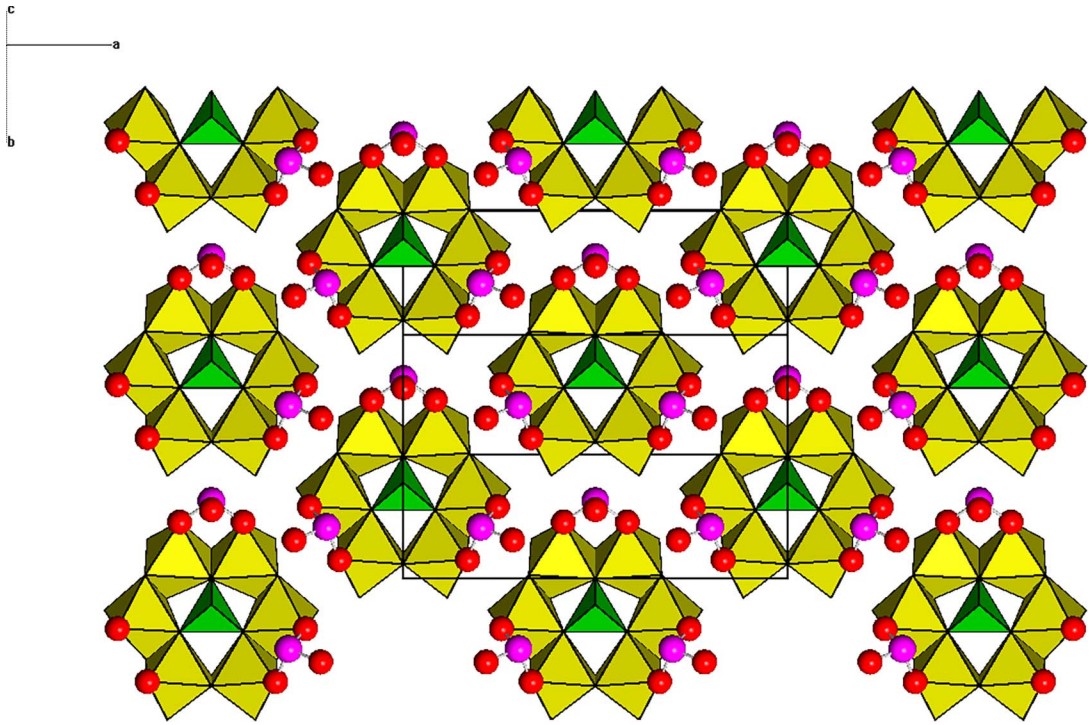

FIG. 5. A layer formed by $[Al(OH)_{3/2}(H_2O)]_6(SeO_3)_3(SiO_3OH)$ cluster structural units in petermegawite. The legend is the same as in Figure 4.

0.138(6) S at the *Se*2 site, yielding a total of 0.38 S *apfu*, which is close to that (0.34 S *apfu*) determined from the electron microprobe analysis. The *Si* site was assumed to be fully occupied by Si without Al, as the X-ray structure analysis is insufficient in distinguishing Si from Al due to their similar X-ray scattering powers. No H atoms were located by the difference Fourier syntheses. All atoms were refined anisotropically. Final refinement statistics for petermegawite are listed in Table 3. Atomic coordinates and displacement parameters are given in Tables 4 and 5, respectively. Selected bond distances are presented in Table 6. All OH and H_2O groups were determined from the bond-valence sums calculated using the parameters given by Brown (2009) (Table 7). The final chemical formula from the structure refinement is $Al_6[(Se_{0.87}S_{0.13})_{\Sigma 1.00}O_3]_3[SiO_3(OH)](OH)_9 \cdot 10H_2O$.

CRYSTAL STRUCTURE DESCRIPTION AND DISCUSSION

The crystal structure of petermegawite is characterized by clusters of six-membered rings composed of edge-sharing AlO_6 octahedra with an $SiO_3(OH)$ tetrahedron situated at the center of each ring and three $Se^{4+}O_3$ triangular pyramids appended outside the ring (Fig. 4). These clusters are joined together by hydrogen bonds to form heteropolyhedral layers parallel to (001) (Fig. 5). The three distinct H_2O molecules (*O*18W, *O*19W, and *O*20W), not bonded to any non-H cations (Al, Se, or Si), are sandwiched between the heteropolyhedral layers. These are linked together by hydrogen bonds (Fig. 6), which accounts for the perfect {001} cleavage of the mineral. It is worth noting that the six-membered rings of edge-shared AlO_6 octahedra in a heteropolyhedral layer do not lie parallel to (001); rather, they are all tilted in the same direction, with their cants being either $+30°$ or $-30°$ with respect to (001) when viewed along [100] (Fig. 7). Moreover, the cants of the six-membered rings alternate their directions from one layer to the next, as shown in Figure 7.

All three symmetrically distinct Al cations in petermegawite have the same octahedral coordination environments: 2O + 3(OH) + H_2O, with similar average Al–O bond distances (<Al1–O> = 1.904 Å, <Al2–O> = 1.899 Å, and <Al3–O> = 1.900 Å) (Table 6), which are very similar to the <Al–O> distance (1.903 Å) for the AlO_6 octahedron in alfredopetrovite (Kampf *et al.* 2016a).

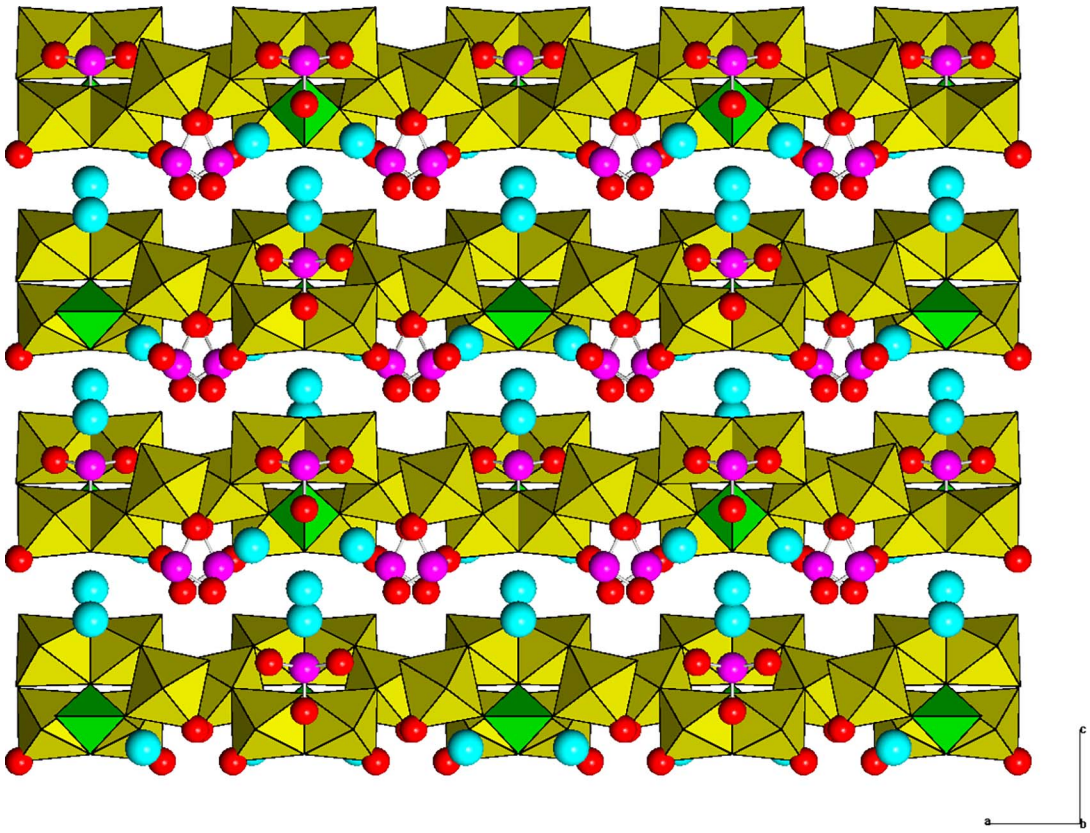

FIG. 6. The crystal structure of petermegawite showing the stacking of heteropolyhedral layers formed by $[Al(OH)_{3/2}(H_2O)]_6(SeO_3)_3(SiO_3OH)$ clusters along [001]. The legend is the same as in Figure 4. The aqua spheres represent H_2O molecules that are not bonded by any non-H cations (Al, Se, or Si).

Silicon is tetrahedrally coordinated by (3O + OH), among which three O atoms are shared with AlO_6 octahedra. Both $Se1O_3$ and $Se2O_3$ triangular pyramids have two O atoms shared with AlO_6 octahedra and the third O atom is unshared, similar to that observed in alfredopetrovite (Kampf *et al.* 2016a). However, both <Se1–O> (= 1.693 Å) and <Se2–O> (= 1.686 Å) in petermegawite appear to be slightly shorter than the <Se–O> distance (1.709 Å) in alfredopetrovite, probably due to the substitution of some smaller S^{4+} (r = 0.37 Å) for Se^{4+} (r = 0.50 Å) (Shannon 1976).

The H atoms in petermegawite could not be located in the refined crystal structure, but the bond-valence (BV) calculations allow an assignment of OH ions and H_2O molecules (Table 7). The possible H bonds calculated from O···O distances are listed in Table 8. Noticeably, significant low BV sums are found for O1 (1.43 *vu*) and O4 (1.42 *vu*), which are the unshared apical O atoms of $Se1O_3$ and $Se2O_3$ triangular pyramids, respectively. These two O atoms are acceptors for multiple H bonds (O1···O12W, O13W, O20W = 2.733, 2.682, 2.826 Å, respectively, and O4···O17W, O19W, O20W = 2.665, 3.020, 3.080 Å).

According to spectroscopic studies on hydrous minerals containing $(SeO_3)^{2-}$ and/or $(SiO_3OH)^{3-}$ (*e.g.*, Ratheesh *et al.* 1997, Frost *et al.* 2006a, b, Matsubara *et al.* 2008, Kasatkin *et al.* 2014, Mills *et al.* 2014, Kampf *et al.* 2016b), the tentative assignments of major Raman bands for petermegawite are given as follows: The broad bands between 2860 and 3700 cm^{-1} are due to the O–H stretching vibrations in H_2O and OH groups. The nature of the broad bands between 2250 and 2700 cm^{-1} is unclear. The small sharp band at 990 cm^{-1} is attributed to the Si–O symmetrical stretching vibrations within the (SiO_3OH) group. The bands at 831 and 745 cm^{-1} are ascribable to the Se–O symmetric and antisymmetric stretching modes,

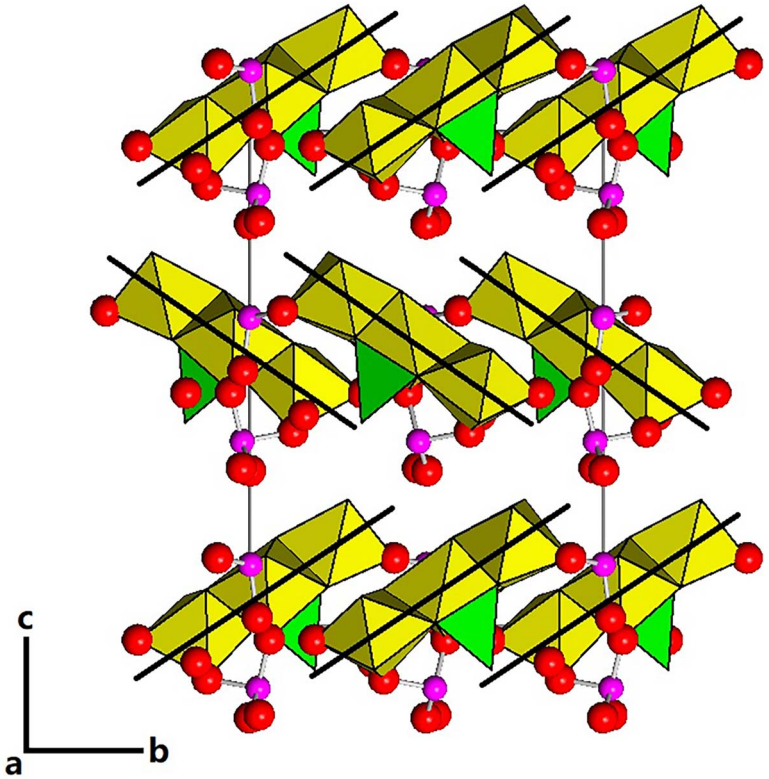

FIG. 7. The crystal structure of petermegawite showing the tilting of six-membered rings of edge-shared AlO_6 octahedra with respect to (001) and the alternation of their cant directions (indicated by black lines) of the six-membered rings from one layer to the next. The legend is the same as in Figure 4.

respectively, within the SeO_3 groups, whereas those from 400 to 650 cm^{-1} originate from the O–Se–O bending vibrations. The bands below 400 cm^{-1} are mainly associated with the rotational and translational modes of SeO_3 groups, as well as the Al–O interactions and lattice vibrational modes.

Chemically, the cluster formed by a six-membered AlO_6 octahedral ring with an SiO_3OH tetrahedron at the center of the ring in petermegawite has the composition $[Al_6(SiO_3OH)O_6(OH)_9(H_2O)_6]^{6-}$. Topologically, it is identical to that found in bettertonite, $[Al_6(AsO_4)_3(OH)_9(H_2O)_5]\cdot 11H_2O$ (Grey *et al.* 2015), and penberthycroftite, $[Al_6(AsO_4)_3(OH)_9(H_2O)_5]\cdot 8H_2O$ (Grey *et al.* 2016), both of which have cluster compositions of $[Al_6(AsO_4)O_7(OH)_9(H_2O)_5]^{8-}$. This type of cluster has recently been recognized as a new polyoxometalate building block seen in the cluster composition of $[VMo_6O_{25}]^{9-}$ (Gao *et al.* 2014). A general chemical formula for such an anionic cluster may be expressed as $[TM_6X_{25}]$, where T = tetrahedrally coordinated cation, M = octahedrally coordinated cation, and X = O, OH, H_2O. Although the heteropolyhedral $[TM_6X_{25}]$ clusters in petermegawite, bettertonite, and penberthycroftite are topologically identical, their linkages are different. In bettertonite and penberthycroftite such clusters are interconnected by corner-sharing with other AsO_4 tetrahedra (not those at the center of six-membered rings) to form undulating layers (Grey *et al.* 2015, 2016), whereas in petermegawite they are only joined together by H bonds to form layers. Nonetheless, the heteropolyhedral layers in all three minerals are linked together by H bonds from interlayer H_2O molecules. There are 11, 8, and 4 interlayer H_2O molecules *pfu* in bettertonite, penberthycroftite, and petermegawite, respectively. Accordingly, to be consistent with the chemical formulae for bettertonite and penberthycroftite, the chemical formula of petermegawite may be better written as $[Al_6(SeO_3)_3[SiO_3(OH)](OH)_9(H_2O)_6]\cdot 4H_2O$ (= heteropolyhedral layer + interlayer H_2O), instead of the originally proposed formula $Al_6(SeO_3)_3[SiO_3(OH)](OH)_9\cdot 10H_2O$.

TABLE 8. POSSIBLE H-BONDING SCHEME IN PETERMEGAWITE

Donor	Acceptor	D–A distance (Å)
O8H	O20W	2.695
O9H	O19W	2.814
O10H	O20W	2.826
O11H	O18W	2.852
O14H	O10H	3.090
O15H	O18W	2.982
O16H	O9H	2.800
O12W	O1	2.733
O12W	O2	2.710
O13W	O1	2.682
O13W	O5	2.706
O17W	O3	2.673
O17W	O4	2.665
O18W	O11H	2.852
O18W	O8H	2.741
O19W	O9H	2.814
O19W	O4	3.020
O19W	O5	3.189
O19W	O20W	3.236
O20W	O8H	2.695
O20W	O1	2.826
O20W	O4	3.080

Acknowledgments

We are grateful for the constructive comments by an anonymous reviewer. This study was funded by the Feinglos family.

References

Brown, I.D. (2009) Recent developments in the methods and applications of the bond valence model. *Chemical Reviews* **109**, 6858–6919.

Frost, R.L., Cejka, J., Weier, M.L., & Martens, W. (2006b) Molecular structure of the uranyl silicates – A Raman spectroscopic study. *Journal of Raman Spectroscopy* **37**, 538–551.

Frost, R.L., Weier, M.L., Reddy, B.J., & Čejka, J. (2006a) A Raman spectroscopic study of the uranyl selenite mineral haynesite. *Journal of Raman Spectroscopy* **37**, 816–821.

Förster, H.-J., Bindi, L., & Stanley, C.J. (2016) Grundmannite, $CuBiSe_2$, the Se-analogue of emplectite, a new mineral from the El Dragón mine, Potosí, Bolivia. *European Journal of Mineralogy* **28**, 467–477.

Förster, H.-J., Bindi, L., Grundmann, G., & Stanley, C.J. (2018) Cerromojonite, $CuPbBiSe_3$, from El Dragón (Bolivia): A new member of the bournonite group. *Minerals* **8**, 420.

Förster, H.-J., Bindi, L., Stanley, C.J., & Grundmann, G. (2017) Hansblockite, (Cu,Hg)(Bi,Pb)Se_2, the monoclinic polymorph of grundmannite: A new mineral from the Se mineralization at El Dragón (Bolivia). *Mineralogical Magazine* **81**, 229–240.

Förster, H.-J., Ma, C., Grundmann, G., Bindi, L., & Stanley, C.J. (2019) Nickeltyrrellite, $CuNi_2Se_4$, a new member of the spinel supergroup from El Dragón, Bolivia. *The Canadian Mineralogist* **57**, 637–646.

Gao, Q., Li, F., Wang, Y., Xu, L., Bai, J., & Wang, Y. (2014) Organic functionalization of polyoxometalate in aqueous solution: self-assembly of a new building block of {VMo_6O_{25}} with triethanolamine. *Dalton Transactions* **43**, 941–944.

Giester, G. & Pertlik, F. (1994) Synthesis and crystal structure of iron (III) selenate (IV) trihydrate, $Fe_2(SeO_3)_3 \cdot 3H_2O$. *Journal of Alloys and Compounds* **210**, 125–128.

Girling, C.A. (1984) Selenium in agriculture and the environment. *Agriculture, Ecosystems & Environment* **11**, 37–65.

Grey, I.E., Kampf, A.R., Price, J.R., & Macrae, C.M. (2015) Bettertonite, $[Al_6(AsO_4)_3(OH)_9(H_2O)_5] \cdot 11H_2O$, a new mineral from the Penberthy Croft mine, St. Hilary, Cornwall, UK, with a structure based on polyoxometalate clusters. *Mineralogical Magazine* **79**, 1849–1858.

Grey, I.E., Betterton, J., Kampf, A.R., Macrae, C.M., Shanks, F.L., & Price, J.R. (2016) Penberthycroftite, $[Al_6(AsO_4)_3(OH)_9(H_2O)_5] \cdot 8H_2O$, a second new hydrated aluminium arsenate mineral from the Penberthy Croft mine, St. Hilary, Cornwall, UK. *Mineralogical Magazine* **80**, 1149–1160.

Grundmann, G. & Förster, H.-J. (2017) Origin of the El Dragón selenium mineralization, Quijarro Province, Potosí, Bolivia. *Minerals* **7**, 1–68.

Grundmann, G., Lehrberger, G., & Schnorrer-Köhler, G. (1990) The El Dragón mine, Potosí, Bolivia. *Mineralogical Record* **21**, 133–150.

Grundmann, G., Lehrberger, G., & Schnorrer-Köhler, G. (2007) The "El Dragón Mine", Porco, Potosí, Bolivia – Selenium minerals. *Mineral UP* **1**, 16–25.

Harrison, W., Stucky, G., Morris, R., & Cheetham, A. (1992) Synthesis and structure of aluminum selenite trihydrate, $Al_2(SeO_3)_3 \cdot 3H_2O$. *Acta Crystallographica* **C48**, 1365–1367.

Holland, T.J.B. & Redfern, S.A.T. (1997) Unit cell refinement from powder diffraction data: The use of regression diagnostics. *Mineralogical Magazine* **61**, 65–77.

Kampf, A.R., Mills, S.J., & Nash, B.P. (2016b) Pauladamsite, $Cu_4(SeO_3)(SO_4)(OH)_4 \cdot 2H_2O$, a new mineral from the Santa Rosa mine, Darwin district, California, USA. *Mineralogical Magazine* **80**, 949–958.

Kampf, A.R., Mills, S.J., Nash, B.P., Thorne, B., & Favreau, G. (2016a) Alfredopetrovite, a new selenite mineral from the El Dragón mine, Bolivia. *European Journal of Mineralogy* **28**, 479–484.

Kasatkin, A.V., Plášil, J., Marty, J., Agakhanov, A.A., Belakovskiy, D.I., & Lykova, I.S. (2014) Nestolaite, $CaSeO_3 \cdot H_2O$, a new mineral from the Little Eva mine, Grand County, Utah, USA. *Mineralogical Magazine* **78**, 497–505.

Kaur, N., Sharma, S., Kaur, S., & Nayyar, H. (2014) Selenium in agriculture: A nutrient or contaminant for crops? *Archives of Agronomy and Soil Science* **60**, 1593–1624.

Lo, K., Wei, J., Zhang, J., & Gu, Q. (1980) Clinochalcomenite, a new mineral of selenite. *Kexue Tongbao* **25**, 427–433.

Lo, K., Chen, Z., & Ma, Z. (1984) The crystal structure of clinochalcomenite. *Kexue Tongbao* **29**, 352–355.

Mandarino, J.A. (1981) The Gladstone-Dale relationship. IV. The compatibility concept and its application. *The Canadian Mineralogist* **19**, 441–450.

Matsubara, S., Mouri, T., Miyawaki, R., Yokoyama, K., & Nakahara, M. (2008) Munakataite, a new mineral from the Kato mine, Fukuoka, Japan. *Journal of Mineralogical and Petrological Sciences* **103**, 327–332.

Mills, S.J., Kampf, A.R., Housley, R.M., Christy, A.G., Thorne, B., Chen, Y.-S., & Steele, I.M. (2014) Favreauite, a new selenite mineral from the El Dragón mine, Bolivia. *European Journal of Mineralogy* **26**, 771–781.

Morris, R.E., Harrison, W.T.A., Stucky, G.D., & Cheetham, A.K. (1991) The syntheses and crystal structures of two novel aluminum selenites, $Al_2(SeO_3)_3 \cdot 6H_2O$ and $AlH(SeO_3)_2 \cdot 2H_2O$. *Journal of Solid State Chemistry* **94**, 227–235.

Morris, R.E., Harrison, W.T.A., Stucky, G.D., & Cheetham, A.K. (1992) On the structure of $Al_2(SeO_3)_3.6H_2O$. *Journal of Solid State Chemistry* **99**, 200.

Paar, W.H., Cooper, M.A., Moëlo, Y., Stanley, C.J., Putz, H., Topa, D., Roberts, A.C., Stirling, J., Raith, J.G., & Rowe, R. (2012) Eldragónite, $Cu_6BiSe_4(Se_2)$, a new mineral species from the El Dragón Mine, Potosí, Bolivia, and its crystal structure. *The Canadian Mineralogist* **50**, 281–294.

Ratheesh, R., Suresh, G., Nayar, V.U., & Morris, R.E. (1997) Vibrational spectra of three aluminum selenities $Al_2(SeO_3)_3 \cdot 3H_2O$, $Al_2(SeO_3)_3 \cdot 6H_2O$ and $AlH(SeO_3)_2 \cdot H_2O$. *Spectrochimica Acta Part A: Molecular and Biomolecular Spectroscopy* **53**, 1975–1979.

Shannon, R.D. (1976) Revised effective ionic radii and systematic studies of interatomic distances in halides and chalcogenides. *Acta Crystallographica*, **A32**, 751–767.

Sheldrick, G.M. (2015a) SHELXT – Integrated space-group and crystal structure determination. *Acta Crystallographica* **A71**, 3–8.

Sheldrick, G.M. (2015b) Crystal structure refinement with SHELX. *Acta Crystallographica* **C71**, 3–8.

Yang, H., Gu, X., Jenkins, R.A., Gibbs, R.B., & Scott, M.M. (2022a) Bernardevansite, IMA2022-057. CNMNC Newsletter 70. *Mineralogical Magazine* **87**, 160–168. DOI: https://doi.org/10.1180/mgm.2022.135

Yang, H., McGlasson, J.A., Gibbs, R.B., & Downs, R.T. (2022b) Franksousaite, $PbCu(Se^{6+}O_4)(OH)_2$, the Se^{6+} analogue of linarite, a new mineral from the El Dragón mine, Potosí, Bolivia. *Mineralogical Magazine* **86**(5), 792–798.

Yankova, R., Genieva, S., Dimov, M., & Nikolova, M. (2021) Analysis and interpretation of interactions in aluminum selenite hexahydrate. *Oxidation Communications* **44**, 1–12.

Received January 16, 2023. Revised manuscript accepted May 19, 2023.

This manuscript was handled by Associate Editor James Evans and Editor Andrew McDonald.